

STUDY OF ENTRANCE CONFIGURATION EFFECT ON STREAMWISE VORTICES IN WAVY CHANNEL

Alexander Christantho Budiman^{1*}, Hatsari Mitsudharmadi², Yann Bouremel³,
Hong Tong Low¹, and Sonny Handojo Winoto⁴

¹ Department of Mechanical Engineering, National University of Singapore, Singapore,
*Tel: +65-8514-7988, e-mail: christantho@u.nus.edu

² Reactive Flow Modeling Laboratory Group in Clean Combustion Research Center,
King Abdullah University of Science and Technology, Thuwal, Kingdom of Saudi Arabia

³ Institute of Ophthalmology, University College London, London, United Kingdom

⁴ Faculty of Engineering, Universitas Diponegoro, Tembalang Campus, Semarang, Indonesia

Received Date: January 1, 2015

Abstract

Two different entrance configurations of a channel with wavy (sinusoidal) surface, namely cosine entrance and negative cosine entrance configuration, were numerically and experimentally investigated to study the downstream development of the induced counter-rotating streamwise vortices. The study is limited to the laminar boundary layer flow. The negative cosine entrance configuration has a “blockage effect” which subjects to large pressure penalty. However, under a certain amplitude and wavelength of the sinusoidal surface, this configuration might have lower hydraulic channel gap than the other configuration due to the formation of separation bubbles at the valley of the sinusoidal surface which makes the stream lifted-up and behaves like a flow in a smooth channel. As such, the flow in the negative cosine entrance configuration is more stable than that in the cosine configuration. This is indicated by the evolution of streamwise vortices at $Re = 2700$ that are preserved farther downstream prior to its breakdown into turbulence.

Keywords: Channel entrance configuration, Hot-wire anemometry, Laminar boundary layer flow, Numerical simulation, Streamwise vortices, Wavy channel

Introduction

Application of surface roughness in fluid mechanics has been widely known for its significant benefits. In turbulence flow aerodynamics, rough elements are installed on the airfoil to delay boundary layer flow separation thus improve the lift of the aircraft. In laminar heat exchanger, surface roughness can be used to improve mixing, control the unwanted disturbance, as well as heat transfer enhancement. However, in both cases, there are additional amount of pressure losses that cannot be ignored, either due to the pressure drag or its geometrical size and shape that accelerates the stream without any pressure recovery [1-4].

One of the benefits of a well-designed surface roughness in plate heat exchangers is its capability to improve mixing without significant pressure drop [5-7]. Surface roughness can be represented mathematically using Fourier expansions as the sum of sinusoidal functions. It is also found that the leading Fourier mode, that is, simple sinusoidal surfaces, could represent various rough surfaces with up to 90% of accuracy and thus, this periodic wavy surface might form the most convenient reference for further study about surface roughness [4, 8].

Given that half of the sinusoidal surface is concave, its centrifugal force could stimulate flow instability in the form of counter-rotating streamwise vortices, which can be distinguished by the variation of streamwise velocity along the spanwise plane. These streamwise vortices are very common in boundary layer flows and are known to be the natural mechanisms of energy dissipation to balance the external forces over the flow. The formation of such streamwise vortices over wavy surfaces might have similarities with the so called Görtler vortices on concave surface laminar boundary layer flows [9, 10]. Furthermore, since the vortical motion from these vortices can potentially be used to enhance mixing in the channel flow, it is important to understand their downstream evolution over the channel with sinusoidal surface. It has been reported that counter-rotating streamwise vortices could preserve longer downstream prior to their breakdown to turbulence in the channel with sinusoidal surface, as compared with the flat plate case [11, 12].

There are at least two different configurations on the transition from flat surface to the wavy surface at the channel entrance, namely cosine and negative cosine, as illustrated in Figure 1. In the previous study, only the negative cosine configuration was used to simulate the pre-set streamwise vortices [13]. The aim of this work is to study the evolution of the streamwise vortices generated by these two different channel entrance configurations in the laminar boundary layer flow. Preliminary numerical simulation results¹, as well as the experimental velocity field measurements, will be presented and discussed.

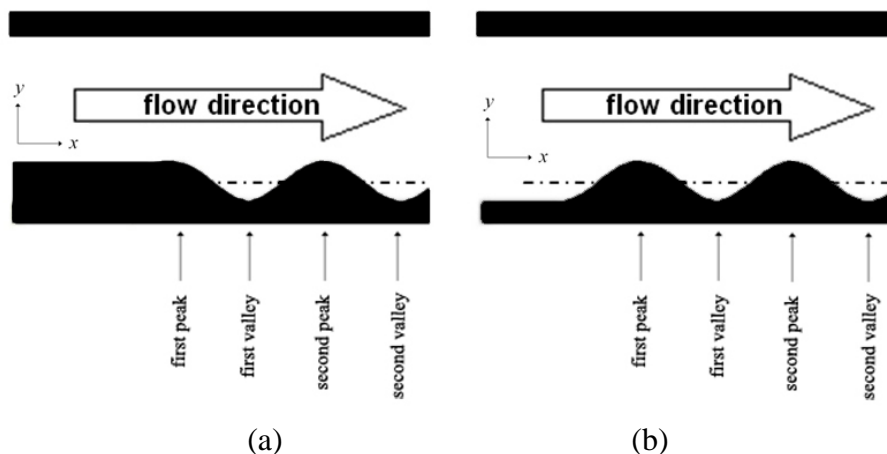


Figure 1. Channel entrance configuration: (a) cosine entrance and (b) negative cosine entrance [13]

Numerical Study

A channel model with rectangular cross-sectional area of 15 mm width by 83 mm height is constructed using GAMBIT 2.4 software. A sinusoidal plate with 3 mm thickness is situated at the center of this channel, connected to a 200 mm length of entrance flat plate. The amplitude a and wavelength of this sinusoidal plate is 3.75 mm and 76 mm, respectively. This geometry gives a dimensionless number $S = a/H = 0.094$, where $H = 40$

¹ The numerical result has been presented in the 7th AUN/SEED-Net Regional Conference in Mechanical and Manufacturing Engineering (RCMME2014), Hanoi, Vietnam, 2014. Phung Lan Huong, editor-in-chief. ISBN: 978-604-911-942-2. Paper number: TE503.

mm is the channel gap. At the leading edge, a jagged triangular cut with 14 mm spanwise length and 6.3 mm depth, respectively, is applied to induce the counter-rotating streamwise vortices with pre-set wavelength. The spanwise wavelength of 14 mm is adapted from the distance between perturbation wires used by Mitsudharmadi *et al.* [14] to pre-set the Görtler vortices with maximum amplification rate. Without this leading edge modification, the natural counter-rotating vortices that could be found at the sinusoidal surface will have non-uniform spanwise wavelength, which might cause difficulties and bias for further study about its downstream evolution [11, 12].

The model is meshed using hybrid Tgrid volume arrangements with uniform edge size of 0.5 mm and imported into FLUENT 14 software for computational simulation. Default transient-k- ϵ -omega, SIMPLE (Semi-Implicit Method for Pressure-Linked Equations), and least squares cell-based are used for flow modeling, pressure-velocity coupling, and gradient discretization, respectively. Air is used as the working fluid. For the boundary conditions setup, all surfaces are set as wall (stationary, no slip), except for the constant velocity inlet, translational periodic side walls, and atmospheric pressure at outlet. The free stream turbulence intensity is set at 0.5%, while the remaining values are set as default. Gravity is excluded in the calculation. The velocity inlet magnitude U_{av} is 2.25 m/s, which corresponds to $Re = U_{av}H/2\nu = 2700$, where H is the channel gap at the channel entrance (parallel flat plate area) and ν is the kinematic viscosity of air. The iterations were performed until the convergence solution is found, that is, the velocity components and continuity residuals were under 1×10^{-4} and 1×10^{-3} , respectively. Prior to the simulation, the accuracy of the calculation using this grid size was verified through a mesh independence test by comparing with various size edges of 0.25, 0.5, 0.75 and 1.5 mm.

Experimental Work

A rectangular channel with one-sided sinusoidal surface with the same size as the numerical model was mounted to an open-loop low-speed wind tunnel. Its maximum free stream turbulent intensity is 0.4% for velocity lower than 5 m/s. However due to the limitation of the experimental setup, the channel gap H was decreased to 35 mm, which corresponds to $S = 0.107$. The sketch of the wind tunnel and the channel (with negative cosine entrance configuration) is shown in Figure 2. The Cartesian coordinates system is used with x , y , and z corresponds to the streamwise, normal, and spanwise direction of the channel, respectively.

Velocity measurements were carried out using hot-wire anemometry. A 1 mm long and 5 μm diameter DANTEC 55P15 tungsten boundary layer hot-wire probe was used to measure the velocity component. The probe is connected to Constant Temperature Anemometer (CTA) and signal conditioner. The system is equipped with traversing mechanism motors that can move in the spanwise and normal direction with accuracy of 0.01 mm. The data acquired was sampled at 6 kHz for duration of 21 seconds and also low-pass filtered at 3 kHz. Calibration checks were performed repeatedly to maintain the acquired data within the range of less than a 2% error.

Results and Discussion

Counter-rotating streamwise vortices with pre-set wavelength in the laminar boundary layer flow have been experimentally generated and numerically simulated by means of the triangle pattern cut at the leading edge. At the center of each triangle pattern, low momentum fluid will be ejected from the wall, creating the upwash region with a thicker

boundary layer. On the other hand, the high speed outer fluid will move towards the wall, resulting in a thinner boundary layer called downwash region [14].

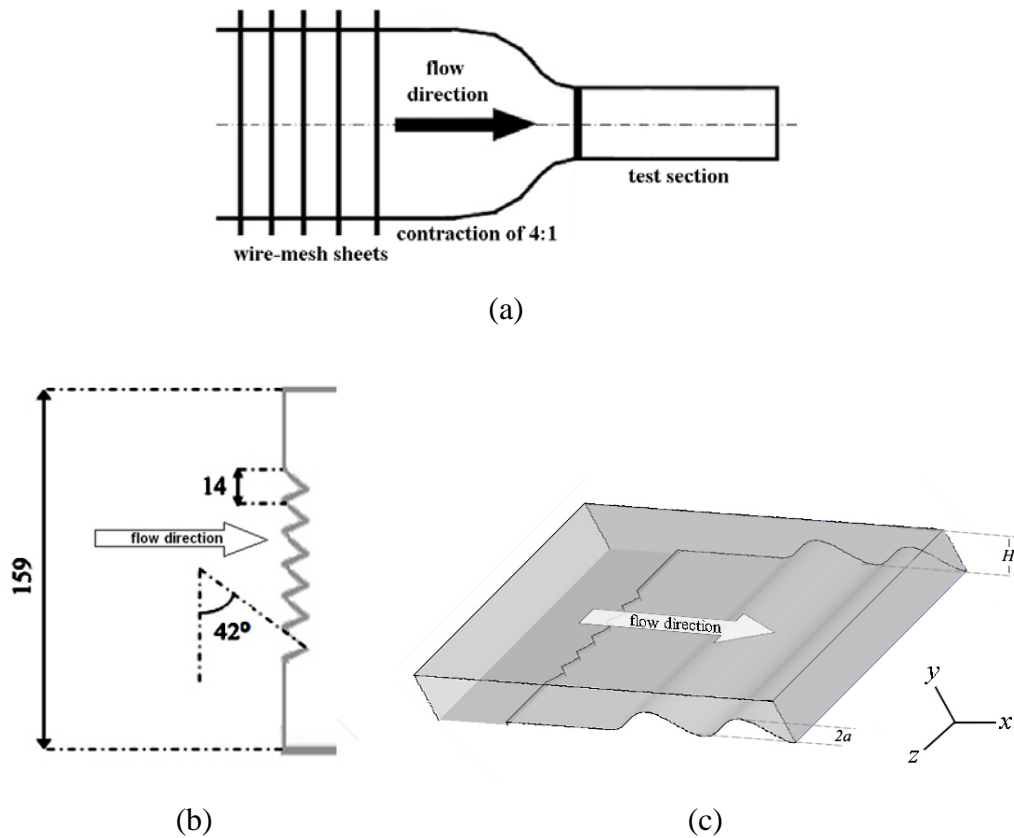


Figure 2. Sketch of (a) the wind tunnel, (b) the jagged pattern on the leading edge (dimensions are in mm) and (c) the wavy channel with negative cosine configuration

The CFD results are presented in Figure 3 and 4. Figure 3 shows the downstream velocity profile at the downwash region which has been normalized by the average velocity at the channel entrance U_{av} . The velocity profile was taken at three different downstream locations, that is, at the vicinity of the leading edge (denoted by the circle in Figure 3), first peak (square), and first valley (triangle) of the sinusoidal surface. The data for further downstream locations are not presented due to the similarities with the velocity profiles in Figure 3.

Due to the thickness of the plate, the flow near the leading edge would slightly decelerate. This happens for both entrance configurations. At the first peak and first valley of the channel with cosine configuration (Figure 3(a)), the velocity profiles u/U_{av} are somewhat more uniform regardless of the y position. The fluid will flow with relatively small acceleration throughout this cosine configuration, compared with the negative cosine configuration. The maximum acceleration that was found above the peak of the wavy surface is around 12.5% higher than the mean entrance velocity. Negative u/U_{av} indicates the separation bubble which occur at $y/H < 0$, while $y = 0$ is the peak of this cosine configuration.

For the negative cosine configuration, substantial acceleration occurs as the fluid approaches the first peak of the wavy surface since the cross-sectional area of the channel decreases (Figure 3(b)). The maximum local velocity magnitude was found to be about

34% higher than the initial velocity set at the inlet of the channel. These maximum values are approximately constant when the fluid enters the valley of the wavy surface.

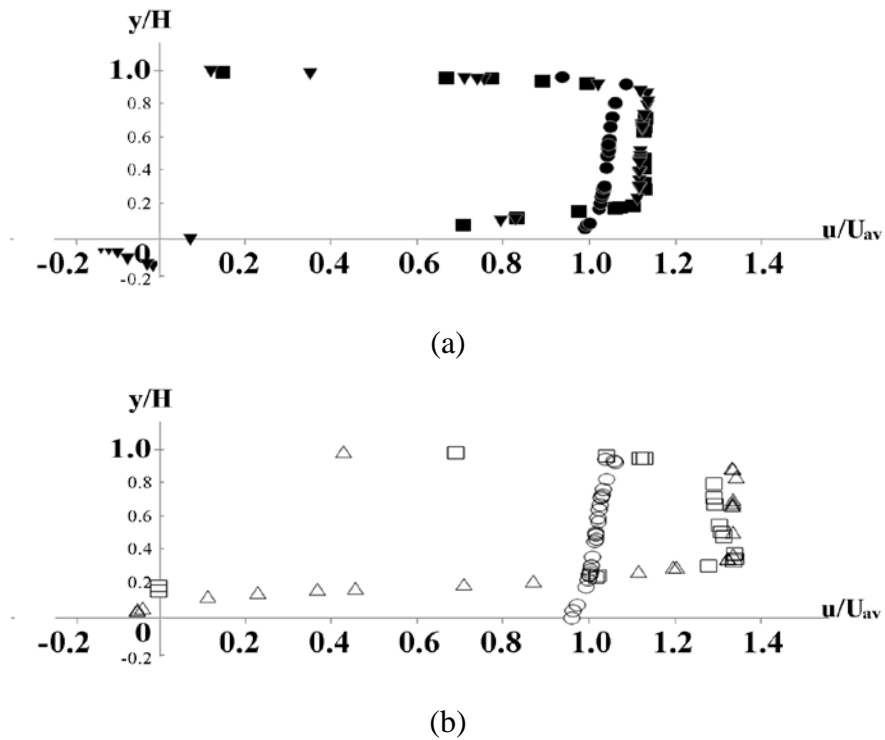


Figure 3. Normalized velocity profile for the downwash region taken at various downstream locations for $Re = 2700$ and $S = 0.094$: (a) for cosine entrance and (b) for negative cosine entrance. Circle indicates the leading edge, square indicates the first peak, and triangle indicates the first valley locations

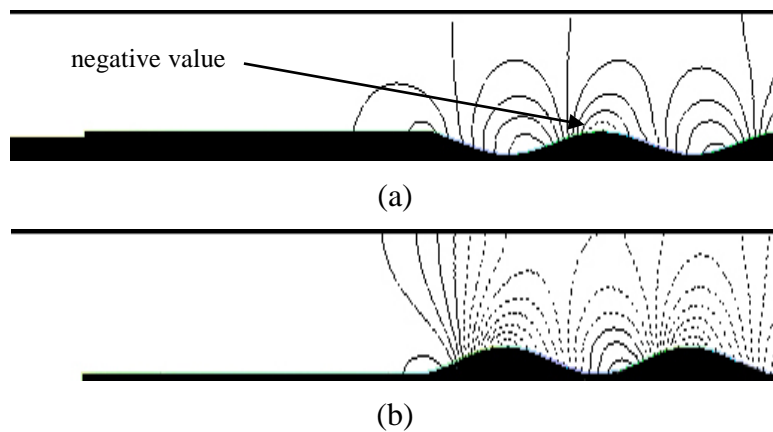


Figure 4. Streamwise pressure contour for $Re = 2700$ and $S = 0.094$: (a) for cosine entrance and (b) for negative cosine entrance. The broken lines represent negative values

In both configurations, a separation bubble was formed in between the two peaks of the sinusoidal surface. The velocity magnitude of the fluid in this recirculation region is negative and significantly lower than the mean velocity. From the visualization by Budiman *et al.* [11], the counter-rotating streamwise vortices structure can still be seen clearly above the first separation bubble region, while after the second peak, the structures

were already diffused. The characterization of the flow in wavy channel with separation bubble would be similar to the Poiseuille flow (flow in the smooth channel) with the hydraulically reduced gap distance [4], since the stream of the fluid is lifted-up above the separation bubble. This explains that negative cosine entrance configuration would have smaller hydraulic channel gap, that is, approximately equivalent to $(H-2a)$, when there is a separation bubble. Conversely, the hydraulic channel gap in the cosine entrance configuration is equal to the actual geometric channel gap H .

Since the stability of the flow is based on this hydraulic gap, it is understandable that the flow in the negative cosine entrance configuration will be more stable than the cosine configuration for the same inlet velocity. However, the negative cosine entrance configuration causes an area reduction in the cross-section area of the wind tunnel test section that is known as “blockage effect”. It causes the flow to accelerate [15] and subsequently produces higher pressure losses, as shown in Figure 4. The broken lines, which are mainly found after the peak of the wavy channel, represent the regions where negative static pressure values are found. In Figure 4(a), the broken lines appeared only near the first peak, while in the negative cosine entrance configuration (Figure 4(b)), the broken lines can be found in almost the entire channel after the first peak.

Experimental results from the measurements using hot wire anemometry are presented in Figure 5 and 6. The appearance of counter-rotating vortices along the y - z plane was not perfectly identical. This might be due to the non-uniformity of the leading edge triangle cut which results in slightly different disturbance amplification rates. However, observation on these vortices can still be done to differentiate the two channel entrance configurations.

Figure 5 shows the plot of normalized streamwise velocity u/U_{av} at the first peak. The data was taken from $-30 \leq z \leq 30$ mm. With 14 mm base length of the jagged leading edge to induce the vortices, it is expected that four counter-rotating streamwise vortices could be found within this spanwise range, according to those presented by Budiman *et al.* [11] and Mitsudharmadi *et al.* [14].

Figure 5(a) shows the velocity profile for the cosine entrance configuration. Although there was a variation of streamwise velocity magnitude, but the minimum velocity from the same y value was not at the upwash region. Without the “blockage effect” from the wavy surface, Figure 5(a) might suggest that the structures were already diffused, similar to the flat plate case [12]. However, this needs to be examined further, for example, by using smoke-wire flow visualization. In contrast, it is shown in Figure 5(b) that the low momentum fluid was located at the upwash region (for example, $z = -8$ and 6 mm). In general, the upwash region tends to be narrow and sharp, while the downwash region occupies wider spanwise range [14, 16]. The maximum u/U_{av} is 1.12 and 1.45 for the cosine configuration and negative cosine configuration, respectively.

According to Mitsudharmadi *et al.* [14], the streamwise vortices could be portrayed as mushroom-like structure in the streamwise velocity contour plotted on the normal plane (y - z plane), where the mushroom stem and mushroom hat represent the upwash and downwash regions, respectively. From the turbulent intensity contour (Figure 6), it is found that the counter-rotating streamwise vortices are only depicted in the channel with negative cosine configuration (Figure 6 (b)). The maximum turbulent intensity is found at the core of the mushroom hat, which is the edge of low momentum streak and corresponds to high shear region [17].

The experimental results show that the flow in the negative cosine entrance configuration is more stable, although only one clear mushroom-like structure can be observed from Figure 6 (b). The contour and magnitude of the turbulent intensity from Figure 6 (a) suggest that the vortices in the cosine configuration were already diffused to

turbulence. Nevertheless, the regions of high fluctuation are still present near the downwash region. Although the parameter S used in the numerical and experimental work is not the same, both studies are qualitatively in good agreement in terms of the evolution of the induced vortices due to different entrance configurations of the channel.

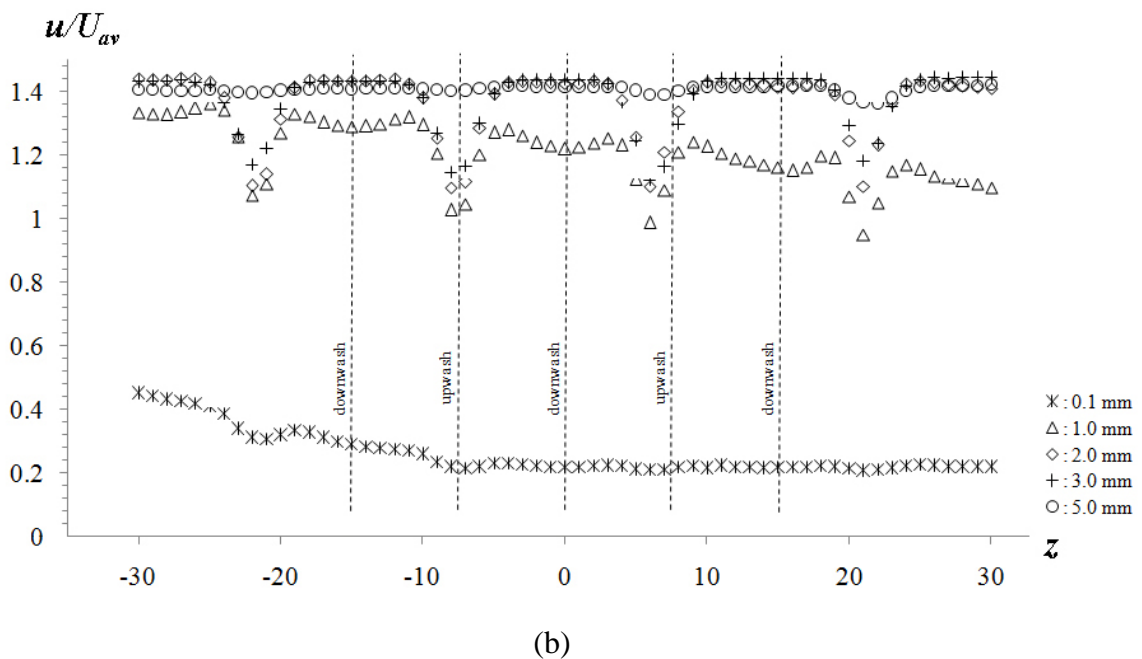
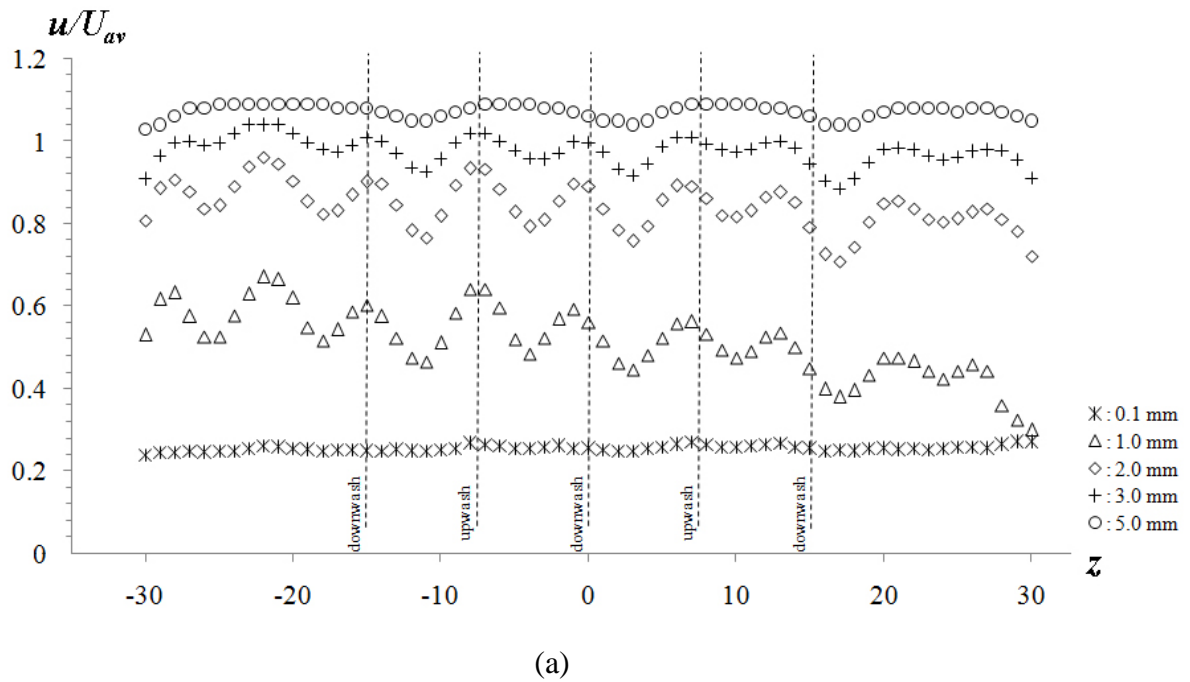


Figure 5. Spanwise distributions of u/U_{av} from the hot wire measurements at the first peak location for $Re = 2700$ and $S = 0.107$ for various normal distances from the sinusoidal surface: (a) for cosine entrance and (b) for negative cosine entrance

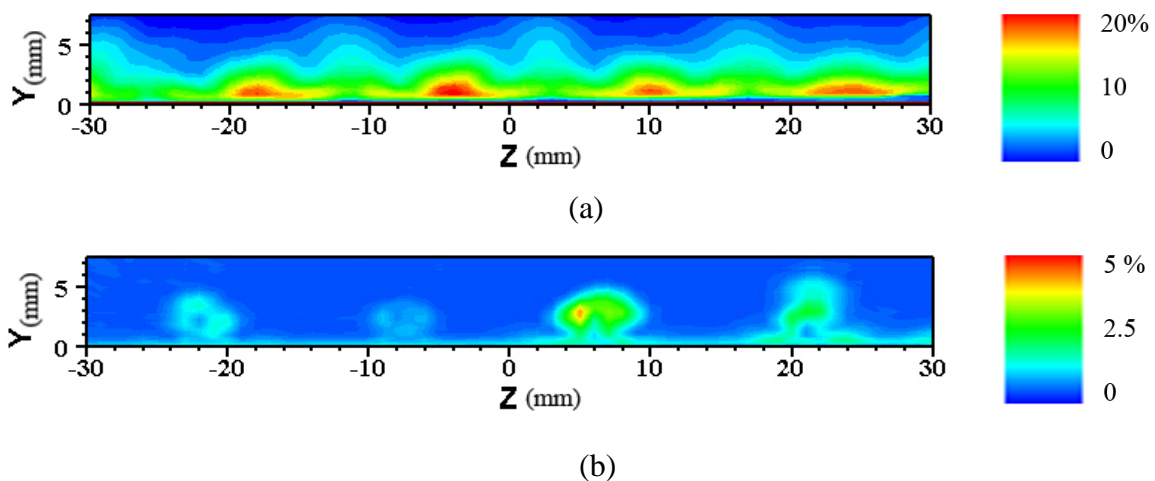


Figure 6. Turbulent intensity contours at the first peak location for $Re = 2700$ and $S = 0.107$ from the hot wire measurements: (a) for cosine entrance and (b) for negative cosine entrance

Conclusions

Numerical and experimental studies on two entrance configurations of a channel with wavy surface, namely cosine entrance and negative cosine entrance, were successfully carried out. These configurations are determined by the connection between the entrance flat plate and the wavy surface. For $Re = U_{av}H/2\nu = 2700$, a notable difference between the two configurations from the flow behavior and vortices structure was found. The negative cosine entrance configuration creates “blockage effect”, which accelerates the mean flow, changes the downstream pressure gradient profile, and also reduces the hydraulic channel gap, making the flow more stable and the vortices remain farther downstream prior to their breakdowns to turbulence. In the cosine entrance configuration, which turned out to have lower pressure penalty, the flow behaves similarly with the plane Poiseuille flow for the same hydraulic channel gap, in which the structure might breakdown significantly earlier.

Acknowledgments

The first author is a recipient of AUN/SEED-Net and NUS Research Scholarship for the Ph.D. Program at the National University of Singapore (NUS).

References

- [1] A. Cabal, J. Szumbariski, and J.M. Floryan, “Stability of flow in a wavy channel,” *Journal of Fluid Mechanics*, Vol. 457, pp. 191-212, 2002.
- [2] E.A.M. Elshafei, M.M. Awad, E. El-Negiry, and A.G. Ali, “Heat transfer and pressure drop in corrugated channels,” *Journal Energy*, Vol. 35, No. 1, pp. 101-110, 2010.
- [3] F. Oviedo-Tolentino, R. Romero-Mendez, A. Hernandez-Guerrero, and B. Giron-Palomares, “Experimental study of fluid flow in the entrance of a sinusoidal channel,” *International Journal of Heat and Fluid Flow*, Vol. 29, pp. 1233-1239, 2008.
- [4] A. Mohammadi, and J.M. Floryan, “Pressure losses in grooved channels,” *Journal of Fluid Mechanics*, Vol. 725, pp. 23-54, 2013.

- [5] P. Gschwind, A. Regele, and V. Kottke, "Sinusoidal wavy channels with Taylor-Görtler Vortices," *Experimental Thermal and Fluid Science Journal*, Vol. 11, pp. 270-275, 1995.
- [6] J.D. Markovic, N.L.J. Lukic, A.I. Jokic, B.B. Ikonc, J.D. Ilic, and B.G. Nikolovski, "2D simulation and analysis of fluid flow between two sinusoidal parallel plates using Lattice Boltzmann method," *Chemical Industry & Chemical Engineering Quarterly*, Vol. 19, No. 3, pp. 369-375, 2013.
- [7] E.A. Bergless, and R.L. Webb, "A guide to the literature on convective heat transfer augmentation," Paper presented at *The 23rd National Heat Transfer Conference*, Denver, United States of America, August 1985.
- [8] M. Asai, and J.M. Floryan, "Experiments on the linear instability of flow in a wavy channel," *European Journal of Mechanics B/Fluids*, Vol. 25, pp. 971-986, 2006.
- [9] J-L. Aider, T. Duriez, and J.E. Wesfreid, "From natural to forced counter-rotating streamwise vortices in boundary layers," *Journal of Physics: Conference Series*, Vol. 137, p. 012009, 2008.
- [10] H. Görtler. "Über eine dreidimensionale Instabilität laminarer Grenzschichten an konkaven Wänden, Ges. D. Wiss. Göttingen," *Nachr. a. d.. Math*, Vol. 2, 1940; translated as "On the three-dimensional instability of laminar boundary layers on concave walls", *NACA TM Vol. 1375*, pp. 1-32, 1954.
- [11] A.C. Budiman, H. Mitsudharmadi, H.T. Low, and S.H. Winoto, "Visualization of counter-rotating streamwise vortices in a rectangular channel with one-sided wavy surface," Paper presented at *The 31st AIAA Applied Aerodynamics Conference (AIAA 2013-2533)*, San Diego, United States of America, June 2013.
- [12] S.M. Hasheminejad, H. Mitsudharmadi, and S.H. Winoto, "Effect of flat plate leading edge pattern on structure of streamwise vortices generated in its boundary layer," *Journal of Flow Control, Measurement & Visualization*, Vol. 2, pp. 18-23, 2014.
- [13] A.C. Budiman, H. Mitsudharmadi, H.T. Low, and S.H. Winoto, "Numerical study on pre-set streamwise vortices in a corrugated channel," Paper presented at *The 6th International Conference on Cooling & Heating Technologies (ICCHT 001)*, Xian, China, 2012.
- [14] H. Mitsudharmadi, S.H. Winoto, and D.A. Shah, "Development of boundary-layer flow in the presence of forced wavelength Görtler vortices," *Physics of Fluids*, Vol. 16, pp. 3983-3996, 2004.
- [15] W.H. Rae, and A. Pope, *Low-Speed Wind Tunnel Testing*, John Wiley & Sons, New York, United States of America, 1984.
- [16] Y. Aihara, and H. Koyama, "Secondary instability of Görtler vortices: Formation of periodic three-dimensional coherent structure," *Transactions, Japan Society for Aeronautical and Space Sciences*, Vol. 24, pp. 78-94, 1981.
- [17] Tandiono, S.H. Winoto, and D.A. Shah, "On the linear and nonlinear development of Görtler vortices," *Physics of Fluids*, Vol. 20, p. 094103, 2008.